JIST 2018, 22 (2): 109-116
ISSN: 2469-9062 (p), 2467-9240 (e)

Research Article

CHARACTERIZATION OF AG:ZNO THIN FILMS AND THEIR USE IN PHOTOELECTROCATALYTIC DEGRADATION OF METHYLENE BLUE (MB)

Bhishma Karki[1*], Jeevan Jyoti Nakarmi[1], Rhiddi Bir Singh[2], Manish Banerjee[3]
[1]Central Department of Physics, Tribhuvan University, Kirtipur, Kathmandu, Nepal
[2]Central Department of Chemistry, Tribhuvan University, Kirtipur, Kathmandu, Nepal
[3]Department of Chemistry, National Institute of Technology, Patna, Patna-800005, Bihar, India
**Corresponding E-mail: magnum.photon@gmail.com*

Received: *28 July, 2017;* ***Revised:*** *25 December, 2017;* ***Accepted:*** *26 December, 2017*

ABSTRACT

The synthesis of functional nano-particles via spray pyrolysis technique (SPT), especially those of catalytic nature, has attracted the interests of scientists and engineers, as well as industries. The rapid and high temperature continuous synthesis yields nano-particles with intrinsic features of active catalysts, that is, high surface area and surface energetic. For these reasons, SPT finds applications in various thermally inducible catalytic reactions. However, the design and synthesis of photocatalysts by SPT requires a knowledge set which is different from that established for thermal catalysts. Unknown to many, this has resulted in frustrations to those entering the field unprepared, especially since SPT appears to be an elegant tool in synthesizing oxide nano-particles of any elemental construct. From simple oxide to doped-oxide, and mixed metal oxide to the in situ deposition of noble metals, this Perspective gives an overview on the development of photocatalysts made by SPT in the last decade that led to a better understanding of the design criteria. Various challenges and opportunities are also highlighted; especially those beyond simple metal oxides, which perhaps contain the greatest potential for the exploitation of photocatalysts design by SPT.

Keywords: Nano-particles, SPT, Photoelectrocatalytic processes, Electron–hole pair, SPR.

INTRODUCTION

ZnO has been extensively investigated as one of the potential semiconductor photocatalyst used in water purification. However, a major limitation to achieve high photocatalytic efficiency in semiconductor nanoparticle systems is the quick recombination rate of photo-induced charge carriers (Karunakaran *et al.*, 2010). To overcome this limitation, one efficient way is to dope noble metals, such as gold, platinum (Li *et al.*, 2012) and silver in the ZnO semiconductors. On the other hand, strong antibacterial activities of both Ag and Ag^+ have been known for a long time (Cho *et al.*, 2011; Khomchenko *et al.*, 2010). ZnO is inorganic antibacterial agent, it can be expected that ZnO will be an excellent support for Ag atoms. In addition, these Ag:ZnO may inhibit the growth of bacteria synergistically due to the strong interaction between them. Keeping these views in mind, we planned to dope silver and gold in ZnO matrix, which not only inhibit photo-corrosion of ZnO electrode but also enhance the degradation of methylene blue (MB) and inactivation rate of the bacteria.

This research deals synthesis and characterization of Ag doped ZnO thin films. Influence of doping concentration onto PEC structural morphological, optical and luminescence properties has been investigated. Moreover large area (100 cm^2) Ag doped ZnO thin films have been prepared on FTO coated glasses (10 – 15 Ω).

MATERIALS AND METHOD

The corning glasses and conducting FTO were used as substrates for Ag:ZnO thin film deposition by spray pyrolysis technique. In thin film deposition process, substrate cleaning is an important factor to get reproducible films as it affects the smoothness, uniformity, adherence and porosity of the films. The substrate cleaning process depends upon the nature of the substrate; degree of cleanliness

required and nature of contaminates to be removed. The common contaminates are grease, adsorbed water, air borne dust, lint, oil particles etc. The corning glasses of dimensions 0.125 cm × 7.5 cm × 2.2 cm and 0.125 cm × 10 cm × 10 cm have been used as substrates. The following process has been adopted for cleaning the substrates.

1. The substrates were washed with detergent solution 'Labolene' and then with water.
2. These substrates were boiled in 0.1 M chromic acid for about five minutes.
3. Substrates were cleaned with distilled water.
4. These substrates were kept in NaOH solution to remove the acidic contaminations.
5. The substrates were again washed with distilled water and cleaned ultrasonically.
6. Finally, the substrates were dried in alcohol (methanol) vapors.

Thereafter, fluorine doped tin oxide (FTO) conducting coatings were prepared onto the corning glass substrates. Initial ingredients (i) Pentahydrated stannic chloride ($SnCl4{\cdot}5H2O$) (purity 99 %), (ii) Ammonium fluoride (NH4F) (99%), (iii) Oxalic acid ($(COOH)2 \times 2H2O$)(99 %) and (iv) Propane-2-ol (Iso-propyl alcohol) (CH3CHOHCH3) (99 %) used to deposit FTO thin films were procured from SD Fine Chem. Mumbai.

A total of 50 ml of 2M stannic chloride (35.7 gm) solution was prepared in doubled distilled water and 7.14 gm of ammonium fluoride was dissolved in it. A few drops of oxalic acid were added to it to clear off some of the precipitated traces. From the above mixture, 10 ml solution was taken and 10 ml of propane-2-ol was added to it to have a total of 20 ml spraying solution.

The final solution was sprayed onto the corning glass substrates of size 0.125 cm × 2.5 cm × 7 cm through the specially designed glass nozzle. The compressed (2.5 kg cm^{-2}) air was used as carrier gas at a constant spray rate of 4.5 ml min^{-1}. The substrate temperature was maintained at 475 ^{0}C. The conducting films thus prepared have sheet resistivity of the order of 5-15 Ω-m and with transparency of 90-95 %. After optimizing all these deposition conditions, FTO films were coated on large area corning glass substrates of size 0.125 cm × 10 cm × 10 cm. These large areas FTO substrates were uniform with resistivity of 5-15 Ω-m at the centre and around 20-30 Ω-m as we go towards its edges. Prior to using FTO as substrates for Ag:ZnO deposition, they were first etched in HCl and finally cleaned with acetone.

Ag:ZnO thin films were deposited onto corning glass and FTO by spray pyrolysis technique. Initial ingredients (procured from Thomas Baker Chem. Mumbai) used to deposit Ag:ZnO thin films were (i) Zinc Acetate ($Zn(CH3COO)2 \cdot 2H2O$, Molecular weight = 219.18 g mol^{-1}) (AR grade, 99.9% pure), (ii) Methanol (CH3OH) (99.9%), (iii) Acetic Acid (99%), and (iv) Silver Nitrate ($AgNO_3$), (99 %).

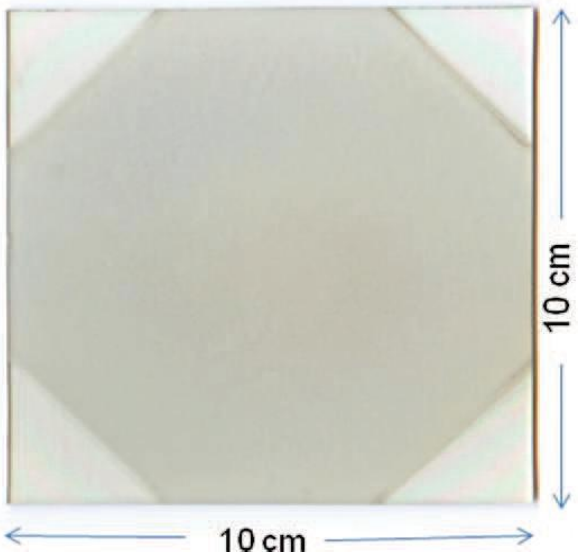

Fig. 1. ZnO thin film on FTO coated glass.

Pure and Ag:ZnO thin films have been deposited onto the ultrasonically cleaned glass substrates using zinc acetate as a precursor solution with the SPT. For growth of pure ZnO thin films, zinc acetate solution was used, while for growth of Ag:ZnO thin film, silver nitrate and zinc acetate precursors were used. An appropriate quantity of silver nitrate (0.2 M) solution was mixed into the zinc acetate solution to accomplish different doping concentrations (i.e. 1, 2, 3 and 4 At %) and subsequently the initial and deposited samples are denoted by ZnO pure, $ZnOAg_1$, $ZnOAg_2$, $ZnOAg_3$, $ZnOAg_4$ respectively. The resulting solution was then pulverized pneumatically by means of a specially designed glass nozzle on to the preheated substrates. The sprayed droplets undergo evaporation, solute condensation and thermal decomposition, thereby resulting in the formation of ZnO thin films. During the synthesis, various preparative parameters like solution quantity (100 ml), solution spray rate (5 ml/min), nozzle to substrate distance (30 cm), carrier gas flow rate (2.5 kg cm^{-1}) etc. were kept at their optimized values. The deposition temperature was kept constant at 400 ^{0}C for the deposition of all samples.

RESULTS AND DISCUSSION

Structural analysis

The X-ray diffraction patterns (C_r Kα", λ= 2.2897 Å) of undoped and silver doped ZnO thin films are shown in Figure 2. The spectrum of undoped ZnO thin film shows typical X-ray diffraction pattern of has hexagonal crystal structure (JCPDS No. 80-0074). Ag can be incorporated in ZnO system either by substitution of Zn^{2+} or by interstitial atom (Lee *et al.*, 2011; Karunakaran *et al.*, 2011; Jin *et al.*, 2011; Xiang *et al.*, 2010). If the silver is substituted for Zn^{2+}, a corresponding peak shift would be expected in XRD. Simultaneously, compared to the (002) diffraction peak of typical undoped ZnO film which located at 2θ= 52.13°, the (002) and that of 1 At % to 4 At % located at, 2θ= 52.15°, 52.17°, 52.18°and 52.23° respectively. Khomchenko *et. al.* (2007), Seetawan *et al.* (2011), Jalalah *et al.* (2013) reported that for 4 wt % silver doped ZnO, the position of (002) was shifted to lower 2θ (0.700°) with increasing Ag dopant, in our case shift is small (0.100°). It is might be due to the segregation of Ag particles in the grain boundaries of ZnO crystallites rather than going into the lattice of ZnO or only an insufficient quantity may be going to substitution Zn site.

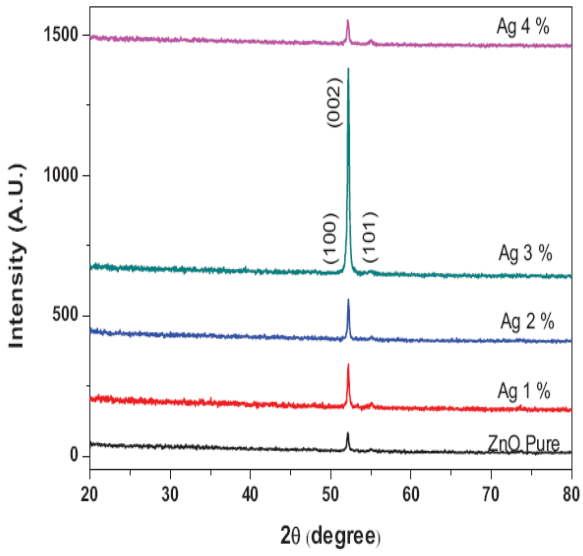

Fig. 2. XRD patterns of undoped and Ag doped ZnO thin films prepared by spray pyrolysis onto glass substrates.

No peaks corresponds to either Ag metal or any of its oxide were observed in the patterns, which indicates that, within the limit of X–ray diffraction no additional phase is present in the Ag:ZnO films. It is evident from XRD analysis and previous reports, the Ag doped ZnO films have preferred orientation along (002) plane (Teoh *et al.*, 2012). Because Ag+ ions have larger ionic radius (0.122 nm) than Zn2+ (0.074 nm), they either substitute ions of Zn2+ leading to the distortion of unit cell or segregate at the grain boundaries of ZnO and hence induced considerable distortion and faster growth of ZnO grains (Khomchenko *et al.*, 2007; Seetawan *et al.*, 2011). Ag+ would preferentially choose to site in the vicinity of grain boundaries due to its larger radius (Myers *et al.*, 2015).

The intensity of the ZnO (002) plane increases with Ag until 3 At % and then decreases with further increase of the Ag which suggest that 3 At % Ag doping can enhance the ZnO (002) preferential orientation but excess Ag doping will deteriorate it. This may be due to the fact that 3 At % Ag quantity of Ag atoms exists an interstitial that share the oxygen with Zn atoms and hence improve the (002) orientation. The excess Ag doping atoms can be energetically favorable to coalesce into metallic silver cluster and hence inhibit c – axis prepared growth of ZnO film.

Morphological properties

The morphology of the ZnO thin films were examined by scanning electron microscopy. Figure

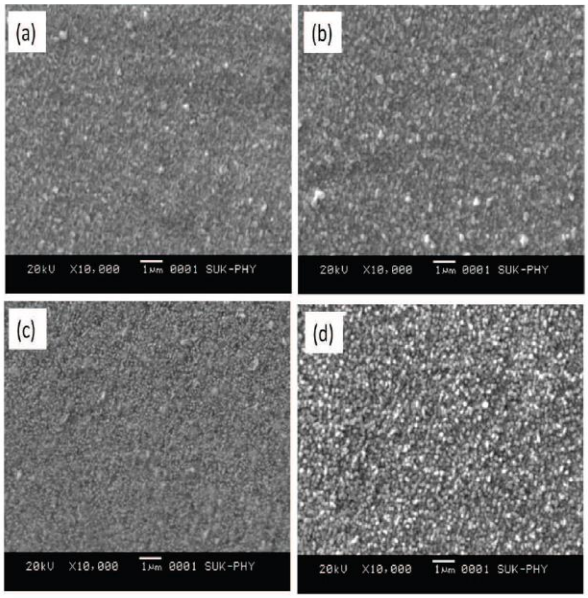

Fig. 3. Scanning Electron micrographs of (a) $ZnOAg_1$, (b) $ZnOAg_2$, (c) $ZnOAg_3$,(d)$ZnOAg_4$.

3 (a-d) shows SEM images of 1 % - 4 % Ag doped ZnO thin films, respectively. The 3 % of Ag doped ZnO thin film shows the smooth surface covered

with grains. The improvement in the grains was observed as Ag doping percentage increases. Average grain size varies from 140 to 166 nm with Ag doping concentration. The surface of 3 At % Ag doping film was found to be hydrophobic (Katoh *et al.*, 2010; Kuang *et al.*, 2016). The chemical composition is determined by the EDAX technique for the ZnO sample deposited at 3 At % Ag doping (figure 4). The values of atomic wt % and mass % of elements are listed in table 1. It has been observed that the atomic wt % of Ag in the film is less than that of starting solution.

OPTICAL PROPERTIES

The optical transmittance spectra for the thin films recorded over wavelength range 300–800 nm at room temperature (figure 5).The sinusoidal nature of transmittance spectra is due to the light interference at the interface between the film and substrate materials. The transmittance of Ag:ZnO films in the visible region decreases from 89 to 74 % as the Ag doping percentage increases. This decrease in the transmittance value of the Ag–ZnO thin films are may be due to the grain boundary scattering. The optical band gap energy (E_g) is an intrinsic property of the semiconductor and is estimated from optical absorption measurement. The optical band gap energy is found to be 3.24 eV for pure ZnO thin films (Subedi *et al.*, 2011; Shieh, *et al.*, 2010; Xu, *et al.*, 2009; Khanlary, *et al.*, 2011), which is comparable to the band gap energy reported by Natsume et al. and for the Ag–ZnO thin films, it is found to be in the range of 3.23 eV. With increasing silver contents, the absorption edge shifted slightly to a longer wavelength region. The band gap also narrowed with increasing Ag contents. Similar results are also observed by Sahu *et al.* (2011).

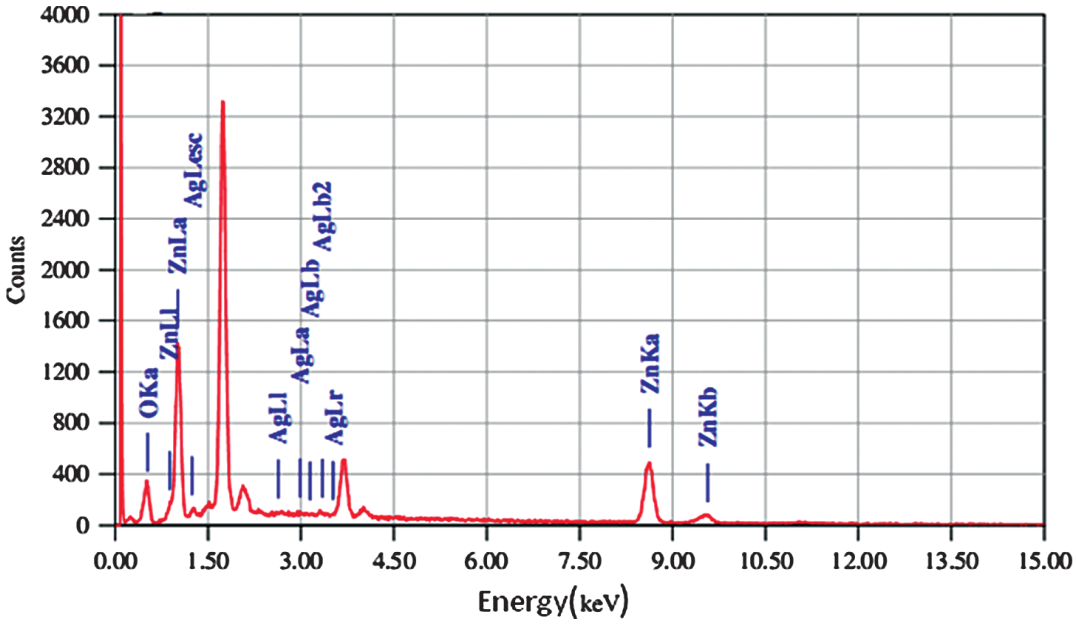

Fig. 4. EDAX pattern of typical 3 At % Ag doped ZnO thin film.

Table 1: EDAX data typical 3 At % Ag doped thin films.

Element	(Mass %)	At %
OK	16.82	46.09
Zn K	82.27	53.55
Ag L	0.91	0.36
Total	100	100

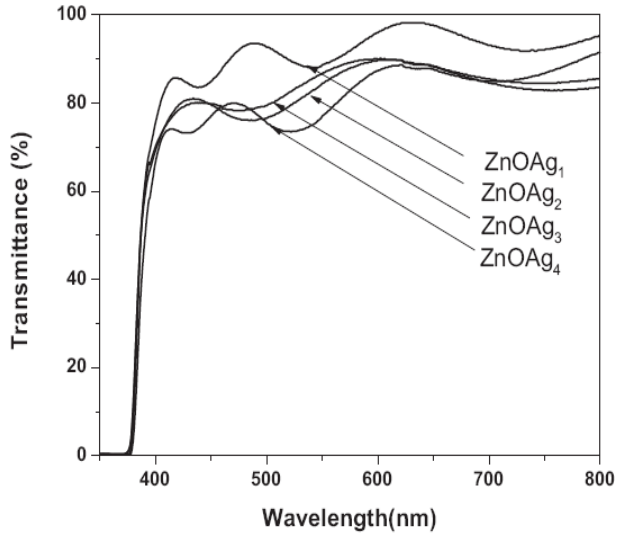

Fig. 5. Optical transmittance spectra of ZnO thin films deposited at various silver doping concentrations.

PHOTOLUMINESCENCE PROPERTIES

The PL spectra of undoped and Ag doped ZnO thin films were recorded at room temperature (Figure 6). Spectra reveal several bands, therefore deconvolution of the spectra was performed assuming the emission peaks to be Gaussian. The deconvoluted spectrum of typical film $ZnOAg_3$ is shown in figure 6 (b).

The UV band related deep- level emission peak, which is observed in ZnO thin films. The new emission peak at about 500 nm is due to Ag doping. The green band in visible region is generally explained by the radiative recombination of the photogenerated holes with electrons and structural defects in crystal.

It might be due to oxygen vacancies and Zn interstitials (Datta *et al.*, 2015). As Ag doping increases in ZnO lattice the excessive cation may generate more anion vacancies and make the concentration of the excitation increases. The Ag^+ ions are substituted for Zn^{2+} ions in the crystal, induced hybridization and charge transfer from a donar – derived impurity band to unoccupied 3d states at the ZnO Fermi level (Holý *et al.*, 2017). The valence of Ag could be assumed to be +1 or/and +2 in the Ag-doped ZnO films. The radius of Ag^+, Ag^{2+} and Zn^{2+} ions are 0.089, 0.072 and 0.122 nm, respectively. So, the Ag^+, Ag^{2+} substitute Zn^{2+} and the Ag^{2+} interstitial might be the main impurity in the Ag-doped ZnO films. The Ag+ substitute was an accepter while the Ag^{2+} interstitial was a donor. When the amount of Ag less than 3 At % in the growth of Ag-doped ZnO films, the concentration of V_{Zn} and Z_{ni} might decrease, this resulted in the weakened blue band. With the increasing of Ag doping, the concentration of Ag^+ substitute and Ag^{2+} interstitial would increase and reach to the maximum, and then would decrease. Z_{ni} might increase with the increasing of the Ag^+ substitute while Z_{ni} defects might increase with the increasing of the Ag^{2+} interstitial because ZnO was a self-assemble oxide compound. So the blue band became strong with the Ag increasing, and reached to the summit when Ag 3 At %, and then decreased (Nebogatikova *et al.*, 2015).

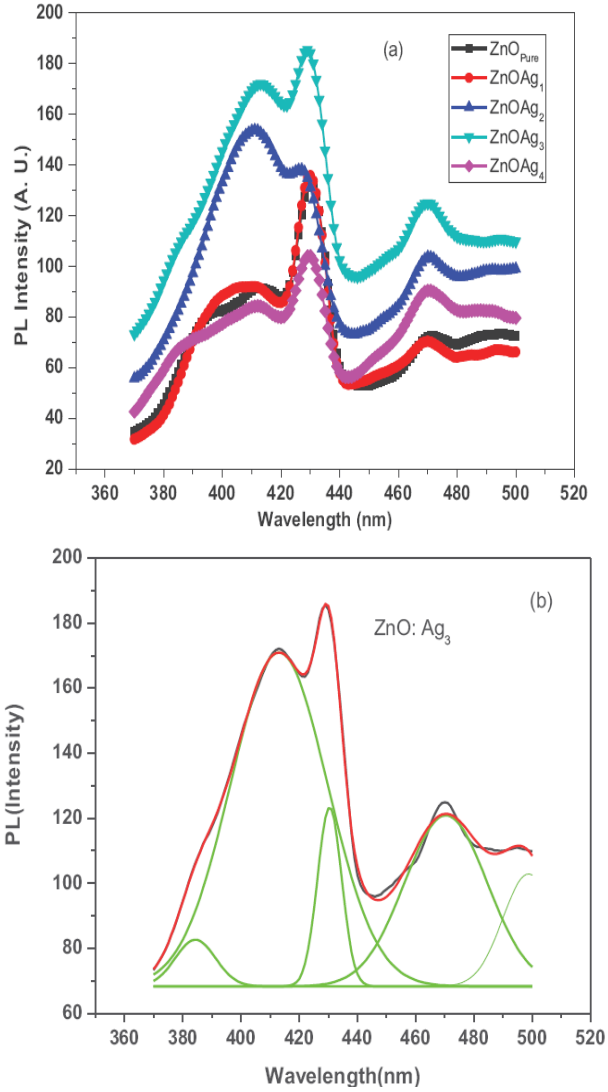

Fig. 6. (a) PL spectra of Ag:ZnO thin films as a function of silver doping percentage. (b) Deconvoluted spectrum of typical ZnO : Ag_3 film.

PHOTOELECTROCHEMICAL (PEC) CHARACTERIZATION

Figure 7 shows variation of I_{sc} and V_{oc} values for different Ag doping concentrations. It is observed that with increasing Ag doping I_{sc} and V_{oc} values increase up to 3 atomic wt % (At %) Ag doping and then decrease for higher concentrations. This consists with the presence of discrete Ag clusters leading to retarded recombination of the photoinduced electron–hole pair and enhanced absorption by Surface Plasmons Resonance (SPR) phenomenon (Sutanto *et al.*, 2015).

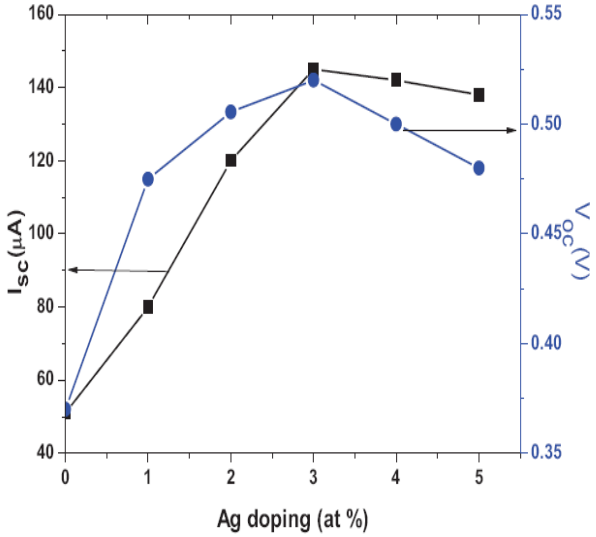

Fig. 7. Variation of I_{sc} and V_{oc} for the PEC cell formed with Ag:ZnO thin film versus Ag doping.

PHOTOELECTROCATALYTIC DEGRADATION OF METHYLENE BLUE (MB)

Effluents from the textile dyeing and finishing industries contain high levels of environmental contaminants, strong color, suspended solids, surfactants and some heavy metals. There are three methods for treatment of colored materials, including (1) physical methods employing precipitation, adsorption, and reverse osmosis; (2) chemical methods via oxidation (using air oxygen; ozone, NaOCl, and H_20_2 as oxidants) and reduction (e.g., $Na_2S_20_4$); and (3) biological methods including aerobic and anaerobic treatment (Ammaih *et al.*, 2014). The disadvantage of precipitation methods is sludge formation. The disadvantage of adsorption is that the adsorbent needs to be regularly regenerated. This is associated with additional costs and sometimes with very time-consuming procedures. Biological treatment is ineffective in cases where complicated aromatic compounds are present. Advanced oxidation processes (AOPs) provide a promising treatment option for textile wastewater compared to other treatment methods (Yan *et al.*, 2006). The advantage of R: ZnO/UVA (R= Ag, Au) photoelectrocatalytic processes is that they prevent any sludge formation during the treatment process. They can be carried out at ambient conditions with the possibility of completely mineralizing organic compound to CO_2. This study was undertaken to evaluate the effectiveness of the R: ZnO/UVA (R= Ag, Au) photoelectrocatalytic process in the decolorization of dye. Methylene blue (MB) was selected as a model dye for photocatalytic degradation using R: ZnO (R= Ag, Au) electrodes.

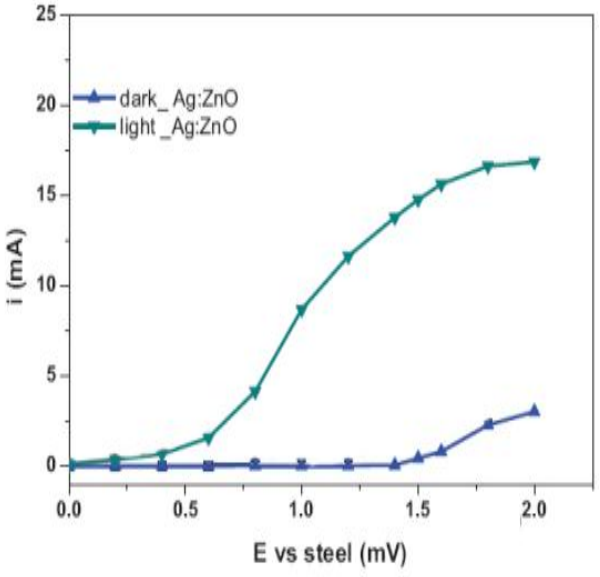

Fig. 8. Dark and light current for Ag:ZnO electrodes (64 cm^2) under UVA illumination for 0.1 M NaOH against applied voltage with respect to steel counter with a flow rate of 12.2 lh^{-1}.

The testing of Ag:ZnO photocatalyst has been carried out by measuring i-E curve. An i-E curve of a 64 cm^2 Ag:ZnO catalyst in 0.1 M NaOH using a steel counter electrode at a distance of 1 mm under UVA illumination is shown in figure 8. The current reached to its saturation value of about 18.7 mA for Ag:ZnO at bias voltage of 1.5 V. The average photocurrent during degradation of MB experiment is 18 mA for Ag:ZnO. In last part of experiment there is slight decrease in photocurrent due to intermediates byproduct formed during photocatalytic reaction. Figure 8.1 shows extinction of MB with reaction time for Ag:ZnO electrode. It

is observed that initial degradation rate is very fast in case of Ag:ZnO electrodes. The percentage of decolorization is calculated using formula,

$$Decolorization\ (\%) = \frac{A - A_0}{A_0} \times 100$$

Where A_0 is absorbance at t = 0 and A is absorbance at time t.

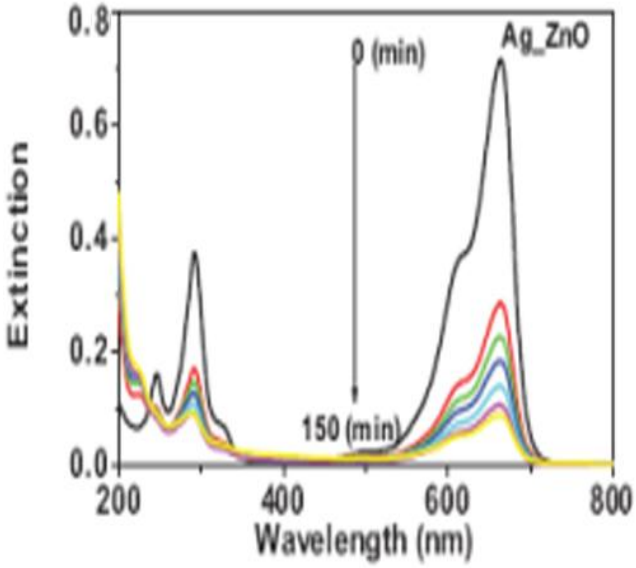

Fig. 8. Extinction spectra of MB with Ag:ZnO under UVA light illumination.

CONCLUSIONS

This paper deals with the characterization of noble metal (Ag) doped zinc oxide thin films. These films have been characterized for their PEC, structural, morphological, compositional and optical properties. The maximum value of Isc and Voc for 3 At % Ag:ZnO thin films confirms the optimization of doping percentage. Films are nanocrystalline and fit well with hexagonal crystal structure with no any extra phases of silver or gold or zinc compounds. For degradation of MB Ag:ZnO films is Used as photoelectrode, it is observed that due to Ag:ZnO 80 % degradation Of MB occurs in 150 min. Photo-corrosion of ZnO electrode is examined by measuring zinc by atomic absorption spectroscopy and no zinc was observed in AAS measurement. The percentage of COD reduction is less than the percentage of decolorization which may be due to the formation of smaller organic compound as reduction of chemical oxygen demand reflects the extent of degradation or mineralization of organic species. Therefore, it requires more time to achieve complete mineralization of MB. From the kinetic parameters and degradation efficiency it is concluded that Ag: ZnO photocatalyst gives better performance in degradation of MB.

REFERENCES

Ammaih, Y.; Lfakir, A.; Hartiti, B.; Ridah, A.; Thevenin, P. and Siadat, M. (2014). Structural, optical and electrical properties of ZnO:Al thin films for optoelectronic applications. *Optical and Quantum Electronics*, **46**: 229–234.

Cho, J. S.; Baek, S. and Lee, J. C. (2011). Surface texturing of sputtered ZnO:Al/Ag back reflectors for flexible silicon thin-film solar cells. *Solar Energy Material and Solar Cells*, **95**: 1852.

Datta, S.; Kaphle, G. C.; Baral, S. and Mookerjee, A. (2015). Study of morphology effects on magnetic interactions and band gap variations for 3 d late transition metal bi-doped ZnO nanostructures by hybrid DFT calculations. *The Journal of chemical physics*, **143** (8): 084309.

Holý, V.; Kriegner, D.; Steiner, H.; Stangl, J.; Bauer, G. and Springholz, G. (2017). High-resolution x-ray diffraction of epitaxial bismuth chalcogenide topological insulator layers, *Advances in Natural Sciences:Nanoscience and Nanotechnology*, **8**: 015006.

Jalalah, M.; Faisal, M.; Bouzid, H.; Ismail, A. A.; Al-Sayari, S. A. (2013). Dielectric and photocatalytic properties of sulfur doped TiO2 nanoparticles prepared by ball milling. *Materials Research Bulletin*, **48**: 3351–3356.

Jin, Y.; Cui, Q.; Wang, K.; Hao, J.; Wang, Q. and Zhang, J. (2011). Investigation of photoluminescence in undoped and Ag-doped ZnO flowerlike nanocrystals. *Journal of Applied Physics*, **109**: 053521.

Karunakaran, C.; Rajeshwari, V. and Gomathisankar, P. (2010). Antibacterial and photocatalytic activities of sonochemically prepared ZnO and Ag–ZnO. *Journal of Alloys and Compounds*, **508**: 587-591.

Karunakaran, C.; Rajeswari, V. and Gomathisankar, P. (2011). Combustion synthesis of ZnO and Ag-doped ZnO and their bactericidal and photocatalytic activities. *Superlattices and Microstructures*, **50**: 234-241.

Katoh, R.; Furube, A.; Yamanaka, K.; Morikawa, T. (2010). Charge Separation and Trapping in N-Doped TiO2 Photocatalysts: A Time-Resolved Microwave Conductivity Study. *The Journal of Physical Chemistry Letters,* **1** (22): 3261–3265

Khanlary, M. R. and Isazadeh, S. (2011). Structural and optical properties of ZnO thin films prepared by sol–gel method. *Micro Nano Letter.,* **6**: 767.

Khomchenko, V. S.; Kryshtab, T. G.; Savin, A. K.; Zavyalova, L. V.; Roshchina, N. N.; Rodionov, V. E. *et al.* (2007). Fabrication and properties of ZnO:Cu and ZnO:Ag thin films. *Superlattices Microstruct,* **42**: 94.

Khomchenko, V. S.; Kushnirenko, V. I.; Papusha, V. P.; Savin, A. K. and Lytvyn, O. S. (2010). Luminescent and structural properties of ZnO-Ag films. *Semiconductors,* **44**: 685.

Kuang, Y.; Jia, Q.; Nishiyama, H.; Yamada, T.; Kudo, A.; Domen, K. (2016). A Front-Illuminated Nanostructured Transparent $BiVO_4$ Photoanode for >2% Efficient Water Splitting. *Advanced Energy Materials,* **6**: 1501645.

Lee, D. H.; Park, K. H.; Kim, S. and Lee, S. Y. (2011). Effect of Ag doping on the performance of ZnO thin film transistor. *Thin Solid Films,* **520**: 1160-1164.

Li, W. J.; Kong, C. Y.; Ruan, H. B.; Qin, G. P.; Huang, G. J.; Yang, T. Y. *et al.* (2012). Electrical properties and Raman scattering investigation of Ag doped ZnO thin films. *Solid State Communications,* **152**: 147-150.

Myers, M. A.; Khranovskyy, V.; Jian, J.; Lee, J. H.; Wang, H. and Wang, H. (2015). Photoluminescence study of p-type vs. n-type Ag-doped ZnO films. *Journal of Applied Physics,* **118**: 065702.

Nebogatikova, N. A.; Antonova, I. V.; Prinz, V. Y.; Kurkina, I. I.; Vdovin, V. I.; Aleksandrov, G. N. (2015). Fluorinated graphene dielectric films obtained from functionalized graphene suspension: preparation and properties. *Physical Chemistry Chemical Physics,* **17**: 13257.

Sahu, D.; Acharya, B. S. and Panda, A. K. (2011). Role of Ag ions on the structural evolution of nano ZnO clusters synthesized through ultrasonication and their optical properties. *Ultrasonic Sonochemistry,* **18**: 601.

Seetawan, U.; Jugsujinda, S.; Seetawan, T.; Euvananont, C.; Junin, C.; Thanachayanont, C. *et al.* (2011). Effect of annealing temperature on the crystallography, particle size and thermopower of bulk ZnO. *Solid State Sciences,* **13**: 1599–1603.

Shieh, J.; Hou, F. J.; Chen, Y. C.; Chen, H. M.; Yang, S. P.; Cheng, C. C. *et al.* (2010). Robust air-like super hydrophobic surfaces. *Advanced Materials,* **22**: 597-601.

Study of morphology effects on magnetic interactions and band gap variations for 3 d late transition metal bi-doped ZnO nanostructures by hybrid DFT calculations

Subedi, D. P.; Madhup, D. K.; Sharma, A.; Joshi, U. M. and Huczko, A. (2011). Study of the Wettability of ZnO Nanofilms. *International Nano Letters,* **1**: 117-122.

Sutanto, H.; Nurhasanah, I. and Hidayanto, E. (2015). Deposition of Ag 2~6 mol%-doped ZnO photocatalyst thin films by thermal spray coating method for E. coli bacteria degradation. *Materials Science Forum,* **827**: 3–6.

Teoh, W. Y.; Scott, J. A.; Amal, R. (2012). Progress in Heterogeneous Photocatalysis: From Classical Radical Chemistry to Engineering Nanomaterials and Solar Reactors. *The Journal of Physical Chemistry Letters,* **3**: 629–639.

Xiang, Q.; Meng, G.; Zhang, Y.; Xu, J.; Xu, P.; Pan, Q. *et al.* (2010). Ag nanoparticle embedded-ZnO nanorods synthesized via a photochemical method and its gas-sensing properties. *Sensors Actuators B: Chemical,* **2**: 635-640.

Xu, M.; Zhao, H.; Duan, M. Y. and Xu, L. X. (2009). Effect of doping with Co and/or Cu on electronic structure and optical properties of ZnO. *Journal of Applied Physics,***105**: 043708.

Yan, X.; Ohno, T. K.; Nishijima, A. R.; Ohtani, B. (2006). Is methylene blue an appropriate substrate for a photocatalytic activity test? A study with visible-light responsive titania. *Chemical Physics Letters,* **429**: 606–610.